

PROCESSING OF NEARLY PURE IRON USING 400W SELECTIVE LASER MELTING – INITIAL STUDY

DAVID PALOUSEK, LIBOR PANTELEJEV, TOMAS ZIKMUND, DANIEL KOUTNY

Brno University of Technology, Faculty of Mechanical Engineering, NETME Centre, Brno, Czech Republic

DOI: 10.17973/MMSJ.2017_02_2016184

e-mail: palousek@fme.vutbr.cz

The proposed article deals with development and initial tests of nearly pure iron powder ATOMET Fe AM (Rio Tinto, QMP) using 400W selective laser melting technology. Magnetic properties in conjunction with 3D printing possibilities of metals could be used in many applications. Metal powder was analyzed for verification of distribution and shape of particles. The main laser parameters such as laser power, laser scanning speed and hatch distance were tested to achieve low porosity and sufficient, high building speed. Laser scanning speed was tested in the range from 200 mm/s up to 1400 mm/s and laser power from 100 W to 400 W. The hatch distance was set to the values of 90, 120 and 150 μm . Porosity was evaluated via microscopy image analysis and micro CT. To obtain mechanical properties the tensile testing was performed.

KEYWORDS

selective laser melting, pure iron, porosity, mechanical properties, pure Fe

1 INTRODUCTION

Selective laser melting is an additive powder bed technology of metals which produces parts from fine metal powder using a high-performance laser beam. Metal parts are built layer by layer directly on the base platform. This technology is suitable for production of geometrically complex parts [Contuzzi 2013], [Yan Chunze]. Also, the microstructure is different if compared with standard materials, and material exhibits higher mechanical properties [Casalino 2015].

Processing of pure metal powders using selective laser melting is quite rare except for the area of engineering applications where the interesting metals are e.g. gold or pure titanium. Khan et al. [Khan, 2010] focussed their investigation on the Selective Laser Melting (SLM) of 24 carat gold (Au) powder with a mean particle size of 24 μm . The 50W continuous wave ytterbium-doped infrared fibre laser in the infrared range from 1070 nm to 1090 nm wavelength was used. The best reached porosity was around 10 % for 50 μm of layer thickness. Further research [Khan, 2014] also showed the high porosity to be predominantly between the layers. Sing et al. [Sing 2016] investigated the effect of designs and process parameters on the dimensional accuracy and compressive mechanical behaviour of titanium cellular lattice structures fabricated by SLM. Fabrication of the samples was implemented on a SLM 250HL machine (SLM Solutions Group AG, Germany) equipped with a Gaussian beam fibre laser, power up to 400 W with a focus diameter of 80 μm .

Song et al. [Song 2013] showed fully dense iron parts fabricated at the laser power of 100 W using different laser scanning speed. The laser source was YLR-100-SM single mode CW Ytterbium fiber laser (1064–1100 nm). A hydrogen-reduced

sponge iron powder, which displays a general multi-prismatic shape, was used.

Kruth et al. [Kruth 2004] dealt with selective laser melting of mixture consisting of 50 wt. % Fe, 20 wt.% Ni, 15 wt.% Cu and 15 wt.% Fe₃P. He used a Rofin-Sinar Nd:YAG laser source with a wavelength of 1.064 μm and a maximum output power of 300 W in continuous mode. A maximum bending strength of 630 MPa was achieved at a material density of 91%.

The main aim of this article is to find mechanical properties for pure iron produced by SLM technique.

2 MATERIALS AND METHODS

2.1 Standard pure Fe characteristics

The general mechanical properties of conventionally processed pure Fe (wrought iron) can be found e.g. in on-line databases and datasheets from producers Goodfellow, Cambridge Ltd., see Tab. 1.

Pure Fe	
Tensile Strength at Break	180-210 MPa
Tensile Yield Strength	120-150 MPa
Young Modulus	120-150 GPa
Boiling point	2750 °C
Density	7,87 g/cm ³
Melting point	1535 °C

Table 1. Mechanical properties (Goodfellow Cambridge Ltd.)

The mechanical properties depend on production process. For example, in the table 2 below, it is possible to find mechanical properties for low-carbon steel. For the exact same alloy AISI 1006 (RioTinto, 0.25-0.40% Mn) the different mechanical properties depending on the process are presented.

Type	Carbon (%)	Dens. (g/cm ³)	YS (MPa)	UTS (MPa)	Elong. (%)
Wrought Cold-drawn	AISI 1006 Carbon <0.08%	7.87	285	330	20%
Wrought Hot-rolled	AISI 1006 Carbon <0.08%	7.87	165	295	30%

Table 2. Mechanical properties of different production processes (RioTinto)

2.2 Powder characterisation

Powder was used in the virgin state directly from the producer and was not additionally sieved or otherwise processed before its processing. The characterization of water atomized Fe powder (Rio Tinto, Canada) was performed using several procedures.

	Producer	Horiba
Median		26.3 μm
Mean Size		27.3 μm
Std. Dev.		8.8 μm
Diameter of Cumulative (%)	D10% - 15 μm D50% - 28 μm D90% - 44 μm D99% - 60 μm	D10% - 16.9 μm D90% - 38.9 μm

Table 3. Particle size distribution

The shape and morphology (see Fig. 2) of particles were analysed using Scanning Electron Microscopy Zeiss Ultra-Plus (SEM). Particle size distribution was measured by Horiba LA-960 laser particle size analyser.

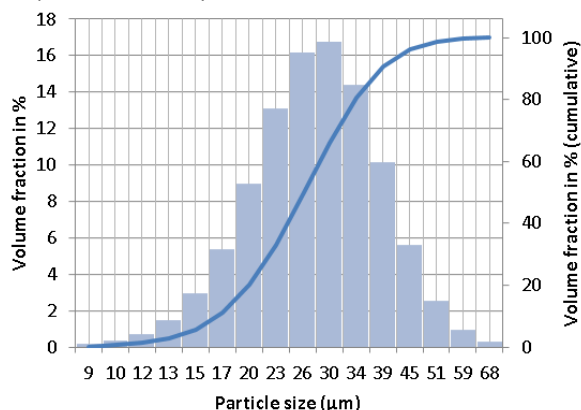


Figure 1. Particle size distribution of pure Fe powder (ATOMET AM)

The powder size distribution declared by producer and our measurement is listed in Tab. 3. The particle size distribution is close to Gaussian distribution (see Fig. 1) and it is suitable for building the layer of thickness between 40 and 60 µm, so the standard thickness layer of 50 µm was used. The particle size distribution analysed by Horiba laser diffraction measurement and declared by producer are slightly different. This discrepancy can be related to specific particle shape (see Fig. 2). A chemical composition of powder guaranteed by the manufacturer is (in weight %): Fe: bal., Mn: 0.04, C: 0.004, O: 0.14, S: 0.008, N: 0.007, P: 0.004, Cu: 0.03, Ni: 0.07, Cr: 0.05.

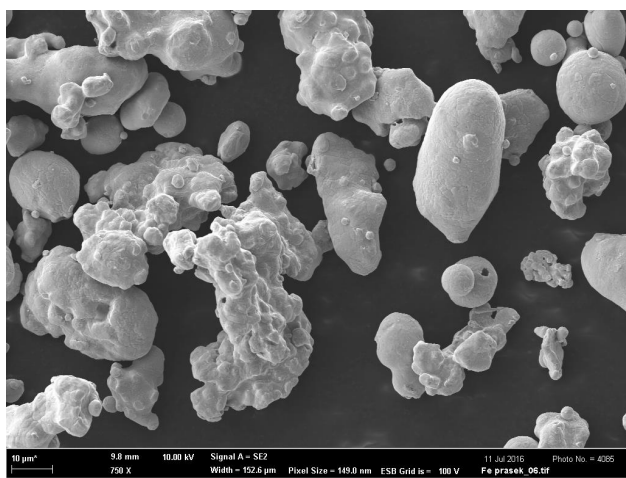


Figure 2. Pure Fe powder, water atomized

The shape of particles is not uniform, which is typical for water atomization, and powder contains round, oval and irregular particles. It can be expected that this could cause problems during the coating process of powder, and then in homogeneity of the powder layer.

2.3 Porosity analysis

For a full raw description of process parameters, sixty cubes (with edge of 5 mm) were built. Laser and process parameters were selected to roughly describe the process window of iron powder. Laser power (L_p) varied in the range of 100, 200, 300, and 400 W, laser scanning speed (L_s) varied in range of 200, 500, 800, 1100, 1400 mm/s. Values of hatch distance (H_d) changed between 90 µm, 120 µm and 150 µm. The constant value of 50 µm of layer thickness (L_t) was chosen.

The laser scanning strategy was identical for all cubes and it is shown in Figure 3, left. Parameters for the contour (red boarder

lines in Fig. 3) and the hatching (black arrows) were also identical. The hatching angle changed over the height of the samples with increment of 90°.

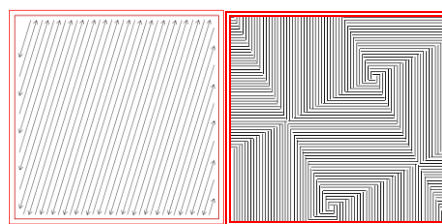


Figure 3. Laser scanning strategy – meander (left), chessboard (right)

For optimizing of process parameters, the second test was performed (see Fig. 4). The samples dimensions of 13×13×6mm were chosen for better understanding of thermal equilibrium. A typical scanning chessboard strategy for larger geometrical structures was used.

A metallographic analysis using light microscopy was used for basic porosity analysis. Samples with low porosity were then selected for microcomputer tomography for detailed porosity observation.

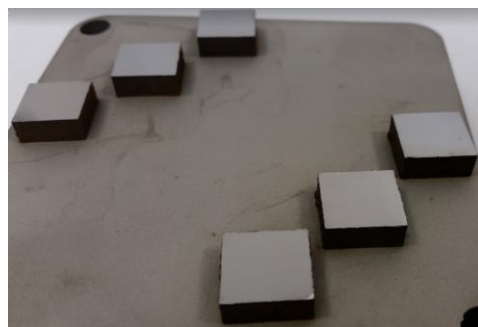


Figure 4. Samples 13x13x6 mm of pure Fe

2.3.1 Micro Computed Tomography (µCT)

The samples were analyzed by micro Computed Tomography (µCT) to obtain the relative porosity and to show the distribution of the cavities in 3D volume. The µCT analysis was performed using the industrial CT system GE phoenix v|tome|x L 240, equipped with a 240kV microfocus X-ray tube and high contrast flat panel detector DXR250 with 2048×2048 pixel, 200×200 µm pixel size. The accelerating voltage was set to 150 kV and the tube current to 55 mA. The exposure time was 600 ms in each of 2200 positions around the 360-degree rotation. Tomographic measurements were performed at the temperature of 21°C. The voxel resolution of obtained CT data was 8 µm. The tomographic reconstruction was realized using software GE phoenix datos|x 2.0 (GE Sensing & Inspection Technologies GmbH, Germany). The porosity analysis and visualization was implemented in VG Studio MAX 2.2.

2.3.2 Metallographic analysis

The samples for microstructural analysis were prepared from SLM tensile billet (13x14x90 mm) in longitudinal and transverse section (with respect to main billet axis). The samples were analyzed by means of a light microscope in etched and non-etched state using metallographic microscope OLYMPUS GX 51.

2.4 Mechanical testing

Tensile testing was performed for evaluation of basic mechanical properties of investigated alloy. SLM samples/billets fabricated with the highest laser speed and low relative porosity were selected for this purpose. Testing samples with nominal diameter of 8 mm and the gauge length of 40 mm were machined from SLM billets (according to DIN

50125). Tensile tests were performed using Zwick Z250 testing machine at room temperature with testing speed of 1 mm/min. Measurement of hardness HV 0.3 was performed using test LECO LM 274 AT hardness tester for evaluation of local mechanical properties. A fractographic analysis was performed on samples broken during tensile tests for assessment of the fracture mechanism of SLM produced iron based alloy.

3 RESULTS AND DISCUSSION

3.1 Porosity

A total of 60 cube samples of 5 mm edge length were fabricated in tree batches for hatch distance 90, 120, 150 μm . All samples were evaluated and compared. The best results were obtained for layer thickness of 90 μm (see Fig. 5)

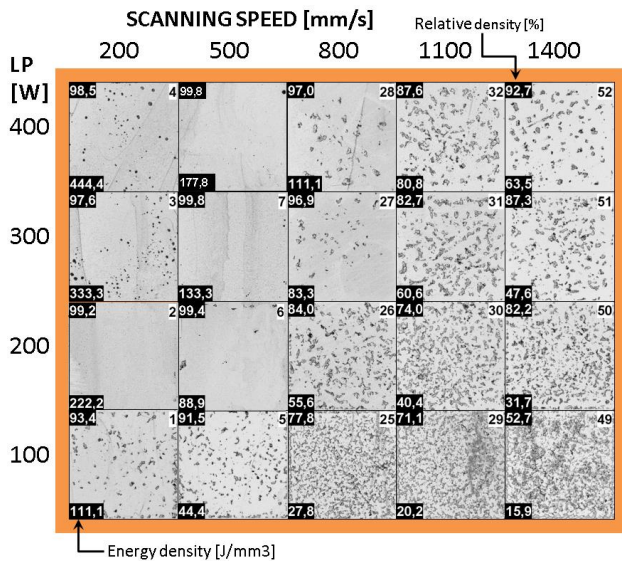


Figure 5. Preliminary analysis of porosity for hatch distance of 90 μm

A small amount of porosity was observed around laser scanning speed of 200 and 500 mm/s (see Fig. 6).

The scanning speed of laser is crucial for economical SLM manufacture. Using of low laser speed leads to a higher manufacturing time consumption and finally to the increase of part cost. Regarding this, low scanning speeds were eliminated from further analysis, and the process window was established between 500 and 800 mm/s and 400 W laser power.

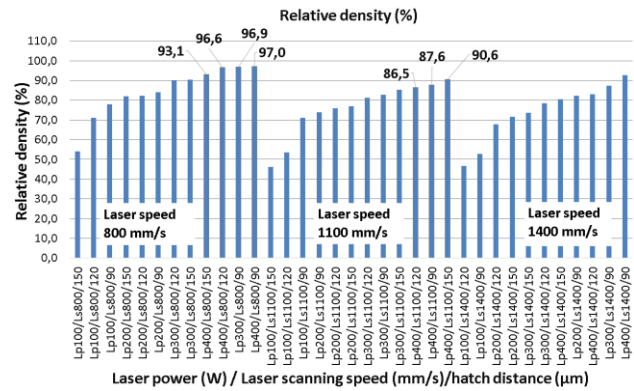
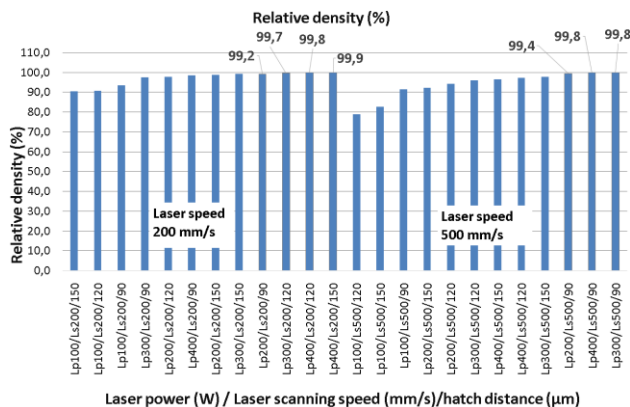


Figure 6. Relative density for 200, 500, 800, 1100 and 1400 mm/s, scanning speed

Next six samples of 13x13x6 mm were manufactured according to the previous outcomes (see Fig. 4). Laser power was set to 400 W and laser scanning speed varied between 500 and 750 mm/s. All samples exhibited a low relative porosity and no cracks were present.

The μCT analysis showed a low number of pores for laser scanning speed in the range between 650 and 750 mm/s, which is suitable for fast speed fabrication. The μCT analysis revealed the volume porosity of 0.15% for laser scanning speed of 750 mm/s (see Fig. 7). To achieve good contrast of μCT images, the sample was machined to size 4x4x10 mm. The process parameters (400 W/750 mm.s⁻¹) were selected to achieve the highest possible productivity of fabrication process. The amount of pores in samples is relatively low regardless irregular shape of the powder particles. Small pores with size up to 8 μm were not detected; however, the total sum of their volumes increases the relative porosity insignificantly.

Voids			
Σ Voxel	538013	Σ PX	7.67 mm ²
Σ Volume	0.27546 mm ³	Σ PY	5.72 mm ²
Σ Surface	38.98 mm ²	Σ PZ	5.83 mm ²
Material			
Iso value	using surface determinator:	Volume	187.19907 mm ³
Voids		0.27546 mm ³	Voids 0.147 %
Inclusions		n/a	Inclusions n/a

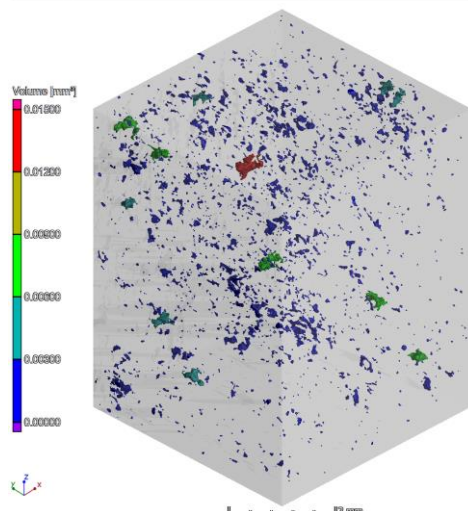


Figure 7. Distribution of voids (μCT analysis) in the 4x4x10 mm sample

3.2 Metallographic analysis

The microstructure of the tensile samples (13x14x90 mm billets, 400 W/750 mm.s⁻¹) in longitudinal and transverse section observed in the non-etched state exhibited the

presence of pores both of spherical and irregular shape with different size (see Fig. 8, 9). The amount of relative porosity is locally higher compared to cube samples, around 0.3% in transverse direction (see Fig. 8) and 2.5% in longitudinal direction.

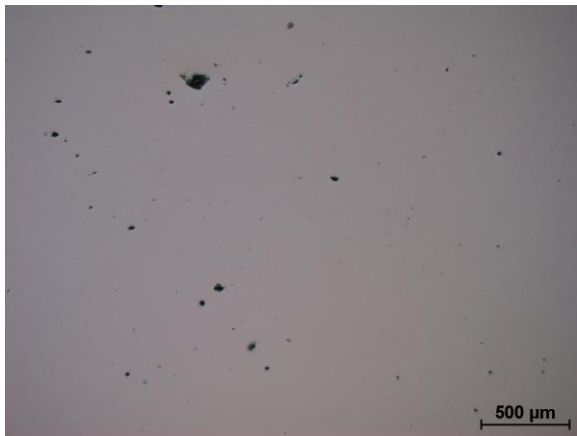


Figure 8. Pores of different shape – transverse direction (non-etched)

The microstructure of investigated SLM iron- base alloy consists of coarser and finer grains with well-defined grain boundaries (see Fig. 10, 11). The arrangement of grains is random, a typical feature of SLM processed materials – the individual welds with fusion boundaries have not been observed. Also, a transition between the consecutive SLM layers was not found.

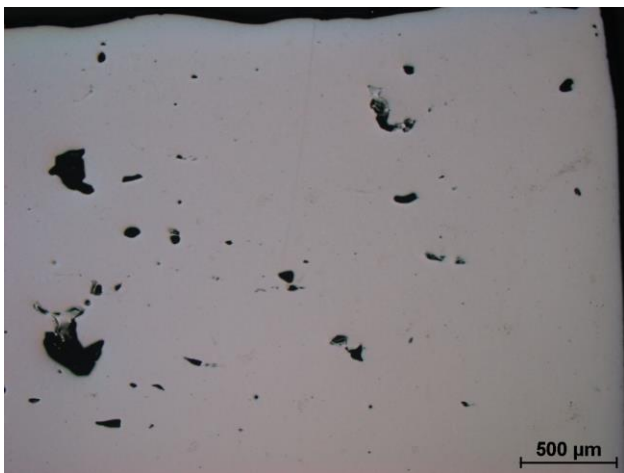


Figure 9. Pores of different shape – longitudinal direction (non-etched)

The microstructure is inhomogeneous; the grain size varies locally between single-digits and tens up to hundreds of microns. Locally, the coarser grains are elongated in the direction of the sample building (see Fig 10, 11). Local mechanical characteristic hardness HV 0.3 was measured on the metallographic sample. The average value calculated from three individual measurements was 143 HV 0.3, wherefrom we can deduce a tensile stress around 467 MPa.

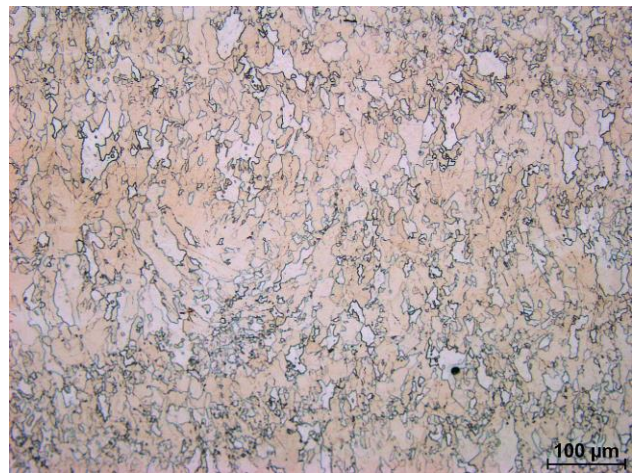


Figure 10. Microstructure of grains – transverse direction (etched)

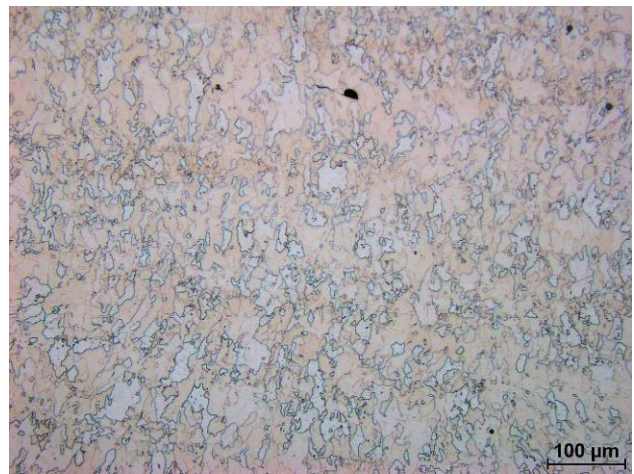


Figure 11. Microstructure of grains – longitudinal direction (etched)

3.3 Tensile test

A tensile test was conducted for evaluation of basic mechanical characteristics. Further listed values are calculated as an average from three individual measurements. The tensile engineering stress-strain curve exhibited discontinuity in the region of yielding, characterized by lower (LYS) and upper yield strength (UYS) respectively (see Fig. 12). The lower yield strength achieved the level of 376 MPa and the upper yield strength of 415 MPa, the ultimate yield strength was 449 MPa and is comparable with the first rough approximation. A strengthening ratio was 1.08 indicating a rather lower level of strain hardening. The percentage elongation at the break was 20 % and the percentage reduction of the area was 56.6 %.

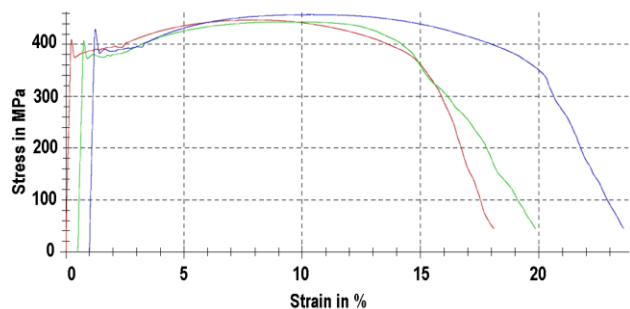


Figure 12. Tensile testing of round tensile samples

These obtained values can be compared with low-carbon steels and it is obvious that the production of parts from pure iron by SLM technique provides very interesting possibilities how to

improve mechanical properties of this material. Compared to Song's SLM iron materials [Song 2013], the tensile strength of 400W SLM-fabricated iron specimens appears higher by 10%. It can be assumed that very small grains in the microstructure assure higher strength due to a large portion of grain boundaries whereas larger grains allow for good plasticity of the material. Strengthening is not probably caused only by grain boundaries, but also by dispersion of oxides present in the microstructure-, because these oxides have already been present in the virgin powder as its natural part. These oxides can act as an effective barrier against a dislocation movement. Oxides present in virgin metal powder cannot be fully removed from the melting pool during the SLM process and persist in the material as an integral part of material microstructure. The fractographic analysis on broken tensile samples was performed for description of fracture mechanism of investigated material. The fracture surface of broken sample is of rough character, a large amount of shrinkage was found (see Fig. 13). Growing of these imperfections copying the layer building is also clearly visible. A detailed analysis revealed a smooth wall of shrinkage with oxide cover and unmelted powder particles inside these imperfections (see Fig. 14). The fracture mechanism is of ductile character with dimple morphology whereas dimples are rather tiny and shallow (see Fig. 15).

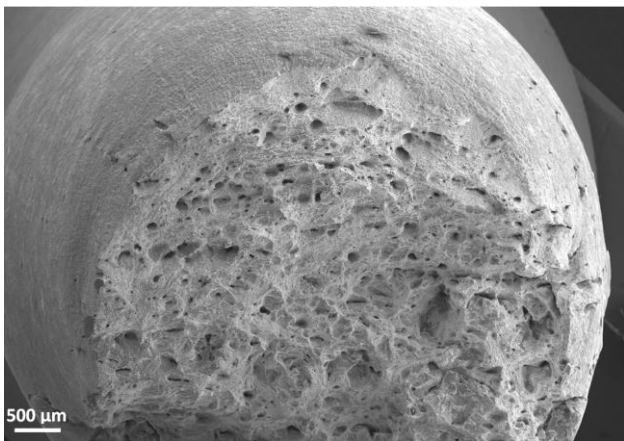


Figure 13. Fracture surface of broken tensile sample

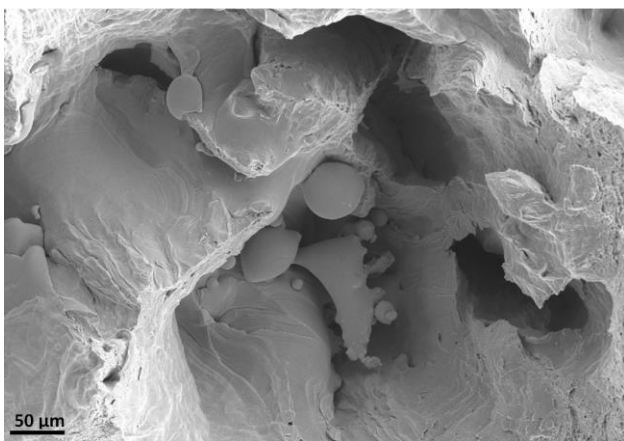


Figure 14. Shrinkage and unmelted powder particles on fracture surface

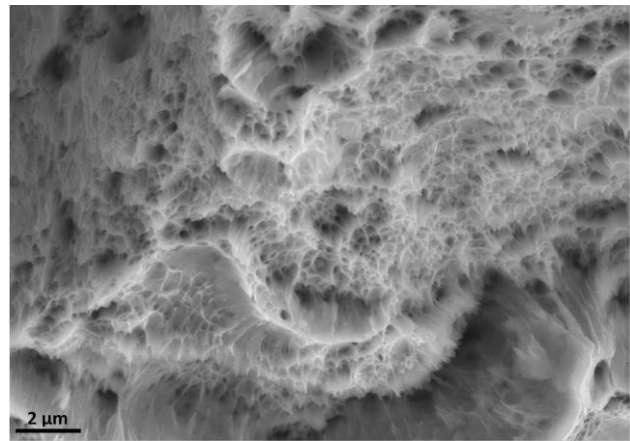


Figure 15. Ductile fracture with dimple morphology

4 CONCLUSIONS

The preliminary study describes the processing of pure iron using a selective laser melting technology. Research focuses on finding the process parameters to minimize porosity and increase the speed of manufacturing.

The study verified the workability of the material without cracks. The microstructure of processed billets is inhomogeneous, consists of grains with different grain size; mechanical properties were found relatively high, ultimate tensile strength of 449 MPa, lower yield strength of 376 MPa and percentage elongation at the break of 20%. The fracture behaviour is of ductile character, whereas the dimple morphology was found on the fracture surface.

The manufacturing speed by SLM technology is critical for the product cost. The laser scanning speed of 750 mm/s was used for the manufacture of tensile specimens with relative porosity that locally varies between 0.3 – 2.5%. Although the porosity is relatively higher, mechanical properties and speed of manufacture predetermine the application of ATOMET FeAT in the area of power and automotive engineering and prototyping.

ACKNOWLEDGEMENTS

The research leading to these results has received funding from the MEYS under the National Sustainability Programme I (Project LO1202). Many thanks to Rio Tinto Metal Powders for material and support.

REFERENCES

- [Casalino 2015] Casalino, G. Experimental investigation and statistical optimisation of the selective laser melting process of a maraging steel. *Optics & Laser Technology*, 2014, vol.65, pp 151-158. ISSN: 0030-3992
- [Contuzzi 2013] Contuzzi, N. Manufacturing and Characterization of 18Ni Marage 300 Lattice Components by Selective Laser Melting. *Materials*, 2013, vol.6, No.8, pp 3451-3468. ISSN: 1996-1944
- [Khan 2010] Khan, M. And Dickens, P. Selective Laser Melting (SLM) of pure gold, *Gold bulletin*, 2010, Vol. 43, No.2., pp 114-121. ISSN 0954-4828
- [Khan 2014] Khan, M. And Dickens, P. Selective laser melting (SLM) of pure gold for manufacturing dental crowns, *Rapid Prototyping Journal*, 2014, Vol.20, Issue.6, pp 471-479. ISSN 1355-2546
- [Kruth 2004] Kruth, J.P., et al. Selective laser melting of iron-based powder, *Journal of Materials Processing Tech.*, 2004, Vol.149(1), pp.616-622. ISSN 0924-0136.
- [Sing 2016] Sing, S. L., et al. Characterization of Titanium Lattice Structures Fabricated by Selective Laser Melting Using an

Adapted Compressive Test Method, Experimental Mechanics, 2016, Vol.56, Issue.5, pp 735-748. ISSN 0014-4851

[Song 2001] Song, Bo., et al. Microstructure and tensile properties of iron parts fabricated, by selective laser melting, October 2013, Vol.56, pp 451-460. ISSN 0030-3992.

[Yan 2012] Yan, Ch. Evaluations of cellular lattice structures manufactured using selective laser melting. International Journal of Machine Tools & Manufacture, 2012, vol.62, pp 32-38. ISSN: 0890-6955

CONTACTS

doc. Ing. David Palousek, Ph.D.

Brno University of Technology

Faculty of Mechanical Engineering

Netme Centre

Technická 2896/2, 616 69 Brno, Czech Republic

Tel.: +420 54114 3261

e-mail: palousek@fme.vutbr.cz

www.3Dlaboratory.cz